

Excited-State Magnetic Properties of Carbon-like Ca^{14+}

Lukas J. Spieß,¹ Shuying Chen^{1,*}, Alexander Wilzewski,¹ Malte Wehrheim¹, Jan Gilles^{1,2}, Andrey Surzhykov^{1,2}, Erik Benkler¹, Melina Filzinger¹, Martin Steinle¹, Nils Huntemann¹, Charles Cheung³, Sergey G. Porsev³, Andrey I. Bondarev^{4,5}, Marianna S. Safronova³, José R. Crespo López-Urrutia⁶, and Piet O. Schmidt^{1,7,†}

¹*Physikalisch-Technische Bundesanstalt, Bundesallee 100, 38116 Braunschweig, Germany*

²*Institut für Mathematische Physik, Technische Universität Braunschweig, Mendelssohnstraße 3, 38106 Braunschweig, Germany*


³*Department of Physics and Astronomy, University of Delaware, Newark, Delaware 19716, USA*

⁴*Helmholtz-Institut Jena, 07743 Jena, Germany*

⁵*GSI Helmholtzzentrum für Schwerionenforschung GmbH, 64291 Darmstadt, Germany*

⁶*Max-Planck-Institut für Kernphysik, Saupfercheckweg 1, 69117 Heidelberg, Germany*

⁷*Institut für Quantenoptik, Leibniz Universität Hannover, Welfengarten 1, 30167 Hannover, Germany*

 (Received 1 March 2025; revised 9 May 2025; accepted 13 June 2025; published 22 July 2025)

We measured the g -factor of the excited-state $^3\text{P}_1$ in Ca^{14+} ion to be $g = 1.499032(6)$ with a relative uncertainty of 4×10^{-6} . The magnetic field magnitude is derived from the Zeeman splitting of a Be^+ ion, cotrapped in the same linear Paul trap as the highly charged Ca^{14+} ion. Furthermore, we experimentally determined the second-order Zeeman coefficient C_2 of the $^3\text{P}_0$ - $^3\text{P}_1$ clock transition. For the $m_J = 0 \rightarrow m_{J'} = 0$ transition, we obtained $C_2 = 0.39 \pm 0.04 \text{ Hz mT}^{-2}$, which is to our knowledge the smallest reported for any atomic transition to date. This confirms the predicted low sensitivity of highly charged ions to higher-order Zeeman effects, making them ideal candidates for high-precision optical clocks. Comparison of the experimental results with our state-of-the-art electronic structure calculations shows good agreement and demonstrates the significance of the frequency-dependent Breit contribution, negative energy states, and QED effects on magnetic moments.

DOI: [10.1103/p88p-brnx](https://doi.org/10.1103/p88p-brnx)

Introduction—Highly charged ions (HCI) have extreme electronic properties as a result of strong internal electric fields, allowing for precise tests of fundamental physics [1,2]. Measurements of atomic parameters of these few-electron HCI are of interest because theory predictions can reach accuracies far beyond what is possible in many-electron systems. In addition, quantum electrodynamics (QED) effects are greatly enhanced due to the high charge state, allowing for stringent tests of QED in the strong-field regime [3]. Furthermore, the response of the atomic structure to a magnetic field B can be both calculated and measured with high accuracy [4–7].

For an electronic level with total angular momentum J and without hyperfine structure, the Zeeman shift from an external magnetic field B is [8]

$$\Delta E_{m_J} = m_J g \mu_B B + g^{(2)}(m_J) \frac{(\mu_B B)^2}{m_e c^2} + \mathcal{O}(B^3), \quad (1)$$

with the magnetic quantum number m_J and the g -factor of the state, the Bohr magneton $\mu_B = e\hbar/2m_e$, the Planck constant \hbar , the electron rest mass m_e , the elementary charge e , and the speed of light c . The second-order Zeeman coefficient $g^{(2)}$ is m_J -dependent with the symmetry relation $g^{(2)}(-m_J) = g^{(2)}(m_J)$.

While investigations of the ground-state g -factor in HCI in Penning traps currently enable the most precise tests of strong-field QED [4], these types of measurements cannot be easily transferred to excited states since the measurement sequence typically takes longer than the excited-state lifetime. Measurements of excited-state g -factors in electron beam ion traps (EBIT) have relative uncertainties on the order of 10^{-4} [9] and thus are larger than those of theory predictions [10]. Our recently developed HCI-based optical clock [11] has enabled measurements of frequencies with sub-Hz precision and of excited-state g -factors with 10^{-6} uncertainty [11,12]. However, the magnetic fields B in those measurements were calibrated relative to the known ground-state g -factor of Ar^{13+} [13]. Knowledge of the Zeeman shifts is also required to obtain unperturbed clock

*Contact author: shuying.chen@quantummetrology.de

†Contact author: piet.schmidt@quantummetrology.de

Published by the American Physical Society under the terms of the [Creative Commons Attribution 4.0 International](https://creativecommons.org/licenses/by/4.0/) license. Further distribution of this work must maintain attribution to the author(s) and the published article's title, journal citation, and DOI.

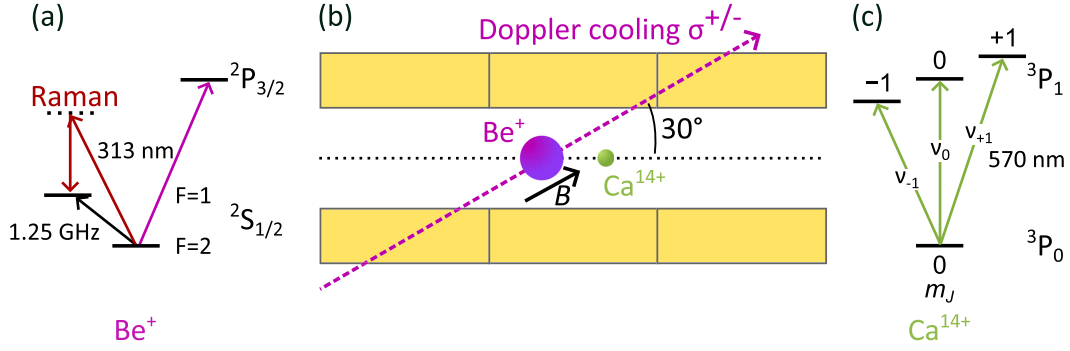


FIG. 1. Sketch of the experimental setup with simplified level schemes of Be^+ and Ca^{14+} . (a) Be^+ with Doppler cooling transition $^2S_{1/2} \rightarrow ^2P_{3/2}$ at 313 nm (purple); hyperfine ground-state $^2S_{1/2}$ transition $F = 2 \rightarrow F = 1$ at 1.25 GHz is driven either by microwaves (black) or a stimulated Raman process (red). (b) Be^+ - Ca^{14+} two-ion crystal confined in a linear Paul trap. The quantization axis at an angle of ca. 30° relative to the symmetry axis of the trap is defined by B as set by three orthogonal pairs of coils (not shown) and optional NdFeB permanent magnets (not shown). The propagation of the Doppler-cooling laser is parallel to B . (c) Simplified level scheme of Ca^{14+} ; $\nu_{-1,0,+1}$ label the Zeeman components of the 3P_0 , $m_J = 0$ to 3P_1 , $m_J = -1, 0, 1$ clock transition at a wavelength of 570 nm.

transition frequencies [2,11]. For clock transitions, the first-order linear Zeeman shift can be averaged to zero [14] by measuring components with opposite m_J . The quadratic terms in the second-order Zeeman shift preclude this procedure, and thus one has to correct for the differential shift $\Delta\nu = C_2(m_J, m_J')B^2$ between the excited (m_J') and ground (m_J) states [15] with

$$C_2(m_J, m_J') = \frac{\mu_B^2}{m_e c^2 h} [g_e^{(2)}(m_J') - g_g^{(2)}(m_J)]. \quad (2)$$

For HCI without hyperfine structure, the sparsity of low-lying energy states due to the large fine-structure splitting should lead to much smaller C_2 than in neutral or singly charged systems [16], but experimental confirmation is so far lacking.

In this Letter, we report on measurements and atomic structure calculations of the excited-state 3P_1 g -factor and $C_2(0, 0)$ of the 3P_0 - 3P_1 transition in Ca^{14+} . Following the experimental approach of Ref. [17], the knowledge of the magnetic field is derived from a cotrapped Be^+ ion. We achieve a relative uncertainty of the Ca^{14+} g -factor of 4×10^{-6} , which, by comparison to calculations, resolves the QED and negative energy eigenstate contributions to g in a system with as many as six electrons. For the calculations, we demonstrate the convergence of the configuration interaction computation in this six-electron system, which enabled us to show the significance of the frequency-dependent Breit contribution to predicting energies of optical transitions in HCI. The small, measured $C_2(0, 0)$ confirms the predicted low sensitivity of HCI to higher-order magnetic field effects. The experimental results provide a test bed for theoretically predicted excited-state magnetic field properties that can easily be transferred to other HCI with optical transitions for the development of high-accuracy HCI clocks.

Experimental setup—A Be^+ and a Ca^{14+} ion are confined together in a cryogenic linear Paul trap [18,19] as sketched in Fig. 1. The Be^+ ion is Doppler cooled using its $S_{1/2} \rightarrow P_{3/2}$ transition at 313 nm. The hyperfine transition at 1.25 GHz between $S_{1/2}$, $F = 2$ and $S_{1/2}$, $F = 1$ is driven either by a microwave (mw) antenna close to the ion trap or by an optically stimulated Raman transition addressing motional sidebands. The frequencies of the hyperfine transitions between the magnetic field-sensitive states $F = 2$, $m_F = \pm 2$ and $F = 1$, $m_F = \pm 1$ are used throughout this Letter to calibrate the magnetic field at the Be^+ position with high accuracy. For this, we numerically invert the Breit-Rabi formula and use the accurately known Be^+ g -factors (for more details about this procedure, see Ref. [20]) [39,40]. All used radio and mw frequencies are referenced to a calibrated H-maser of PTB.

Production, recapture, and cooling of HCI are described in our previous work [41–43]. In brief, a single Be^+ ion cotrapped with an HCI provides sympathetic cooling and enables quantum logic spectroscopy of the latter with sub-Hz precision [12,44]. A Ca^{14+} - Be^+ two-ion crystal has a lifetime of around 2 hours, limited by charge exchange collisions. Loading and preparation of the crystal typically take around 5 minutes. The temperature of all motional modes is < 1 mK [11,12,42]. Here, we study $^{40}\text{Ca}^{14+}$ with an optical transition $^3P_0 \rightarrow ^3P_1$ at 570 nm that features an excited-state lifetime of 11 ms. In an external magnetic field, its three Zeeman components 3P_0 , $m_J = 0 \rightarrow ^3P_1$, $m_J = 0, \pm 1$ have $\nu_{0,\pm 1}$ transition frequencies [see Fig. 1(c)]. These transitions are interrogated with a laser that is stabilized [45] to an ultrastable silicon cavity “Si2” [46] with an optical frequency comb.

The quantization axis is defined at an angle of approximately 30° relative to the symmetry axis of the trap by a magnetic field B , as shown in Fig. 1(b). The direction of B is aligned to a fixed $\sigma^{+/-}$ -polarized laser beam that

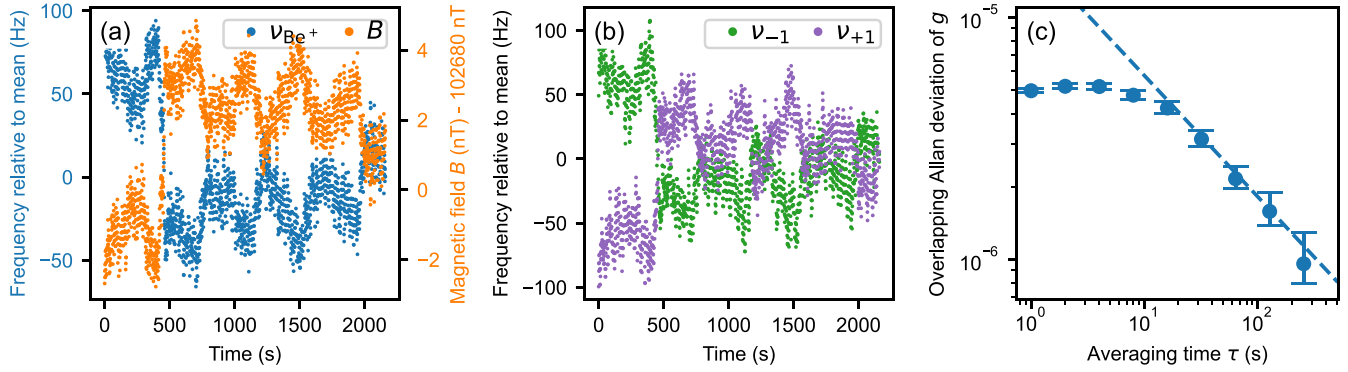


FIG. 2. (a): Frequency deviation of the hyperfine transition ν_{Be^+} in Be^+ (blue) and the derived magnetic field B_{Be} (orange). Oscillations at a period of 6 min are caused by variations of the temperature in the laboratory, which leads to variations of the magnetic field at the ion position (for the lab temperature correlation with the magnetic field at ion position, see Supplemental Material [20]). These effects cancel out when calculating the g -factor. (b) Frequency deviations of the magnetic field-sensitive transitions ν_{-1} (green) and ν_{+1} (purple) in Ca^{14+} . From the data shown in (a) and (b), the g -factor is derived using Eq. (3). (c) Relative measurement instability of the g -factor quantified by the overlapping Allan deviation. The dashed line is a fit $\propto \tau^{-1/2}$, as expected from quantum projection noise for long averaging times.

performs Doppler cooling and state detection of the Be^+ ion. Three orthogonal pairs of coils set the magnetic field direction and strength between $-160 \mu\text{T}$ and $350 \mu\text{T}$. Here, the sign of the B -field indicates its direction relative to that of the laser propagation. For stronger fields up to 1.7 mT , a pair of NdFeB permanent magnets are placed symmetrically around the exit port of the Doppler-cooling beam. The static magnetic field is actively stabilized using a commercial fluxgate magnetometer outside the vacuum chamber and an additional set of compensation coils [18], reaching a fractional instability of 10^{-5} for up to 100 s at the ion position.

g -factor of the $^3\text{P}_1$ state—The g -factor of the $^3\text{P}_1$ state is derived from the first-order Zeeman shift in Ca^{14+} through monitoring of $\nu_{\pm 1}$ while measuring B through the hyperfine transition in Be^+ . The magnetic field at the position of the Ca^{14+} ion is obtained from that at the Be^+ position B_{Be} [40] and a correction for its gradient along the trap axis $b_z = dB/dz$ with

$$g = \frac{h(\nu_{+1} - \nu_{-1})}{2\mu_B(B_{\text{Be}} + b_z d)}. \quad (3)$$

The Ca^{14+} - Be^+ distance d is derived from measurements of the axial motional frequencies of the Be^+ - Ca^{14+} crystal (for details about the measurements and calculations of d , see Supplemental Material [20]) [12,18,21–26].

The field gradient $b_z = 0.30(2) \text{ nT } \mu\text{m}^{-1}$ was determined by moving a Be^+ ion along the axial symmetry axis of the trap and probing the mw transition to determine the magnetic field. We also probe at different radial positions because varying transverse electric fields lead to charge-to-mass ratio-dependent radial displacements, tilting the Ca^{14+} - Be^+ crystal axis with respect to the

symmetry axis of the trap [47], which is the dominant uncertainty of b_z . Further details are given in Supplemental Material [20]. All parameters of Eq. (3), except for b_z , are measured in parallel.

Data obtained under typical operating conditions of $B_{\text{Be}} \approx 103 \mu\text{T}$ and $d \approx 20.4 \mu\text{m}$ are shown in Fig. 2. In Fig. 2(a), the deviations of the Be^+ hyperfine transition frequency from its mean and the derived magnetic field are shown. Figure 2(b) shows the recorded frequency deviation of ν_+ and ν_- in Ca^{14+} in relation to their mean frequency. Additionally, simultaneous measurements of the motional frequency yielded a time-resolved value for d (see Supplemental Material [20]). The overlapping Allan deviation of the g -factor is shown in Fig. 2(c), which shows an instability as expected from white-frequency noise for long averaging times. We assume such a behavior in the entire dataset for determining its statistical uncertainty.

Two independent runs yield a mean value of $g = 1.499032(6)$ with a relative uncertainty of 4×10^{-6} . The error budget is shown in Table I. The largest contribution arises from the magnetic field gradient. Installation of gradient compensation coils could reduce the uncertainty to the low 10^{-7} level in the future, where the accuracy of the ground-state hyperfine structure of Be^+ will become the limiting factor. We have measured the trap drive-induced ac magnetic field [48–50] and determined its influence on the g -factor measurement to be negligible. Time dilation shifts in ν_{\pm} measurements from residual ion motion are common-mode suppressed, and these shifts are negligible for the mw transition in Be^+ due to the long wavelength.

C_2 coefficient—For the measurement of $C_2(0,0)$ in Ca^{14+} , we employ the first-order magnetic field-insensitive transition $^3\text{P}_0, m_J = 0 \rightarrow ^3\text{P}_1, m_J = 0$ with the transition frequency ν_0 . The frequency shift of ν_0 is $\Delta\nu_0 = C_2(0,0)B^2$. We measured ν_0 in four magnetic fields from

TABLE I. Summary of g -factor measurement uncertainties.

Source	Uncertainty/ 10^{-6}
Gradient	6
Statistics	0.4
Be ⁺ atomic parameters	0.2
Trap drive-induced ac Zeeman	< 0.1
Ion-ion distance	< 0.1

25 μT to 1.65 mT using a Yb⁺ single-ion optical clock as a reference [11,51]. For the two largest magnetic field measurements, we employed additional NdFeB magnets attached to one side of the vacuum chamber. The measurements of ν_0 were performed for at least 15 000 s, and reached a statistical uncertainty of approximately 100 mHz for each magnetic field setting. The magnetic field strength B is again obtained from the hyperfine transition frequency measurement in Be⁺. We have confirmed experimentally that, despite the larger magnetic field gradient here, B_{Ca} agrees with B_{Be} to better than 1% (see Supplemental Material for further experimental details [20]). Thus, the corresponding gradient correction is negligible in comparison to the statistical uncertainty of the frequency measurements.

The frequency shift $\Delta\nu_0$ of the Ca¹⁴⁺ clock transition at different magnetic field strengths is shown in Fig. 3. A quadratic fit of the form $\Delta\nu_0 = C_2(0,0)B^2$ yields $C_2(0,0) = 0.39 \pm 0.04 \text{ Hz mT}^{-2}$, where the uncertainty is derived from the fit. The systematic uncertainty from shifts of the Ca¹⁴⁺ clock transition, the reference clock [51], the frequency comb, and other parts of the frequency chain are negligible.

Assuming our typical dc magnetic field of 25 μT for Ca¹⁴⁺ clock operation [42], the measured $C_2(0,0)$ yields a fractional shift of $4.6(5) \times 10^{-19}$.

Theory—The measured atomic parameters are compared with atomic structure calculations. This requires the calculation of transition energies as an essential quality test of the wave functions used to compute the g -factors. The calculations are performed using a large-scale configuration interaction (CI) method to correlate the six electrons following Refs. [52–54]. We converge the CI computation, including excitations up to $24spdfghi$ and extrapolating contributions of higher partial waves. QED corrections are calculated according to Ref. [55]. The results of the computations are listed in Table II. We find an unexpectedly large contribution of the frequency-dependent Breit interaction corrections, which is listed separately in the table. Our calculations show that frequency-dependent Breit contributes at the level of 1% to the Breit interaction, enabling us to estimate for which cases frequency-dependent Breit contributions should be computed to achieve the expected accuracy in future HCI computations. The resulting theoretical energy values are in excellent agreement with the experimental values, as shown in Table II. The

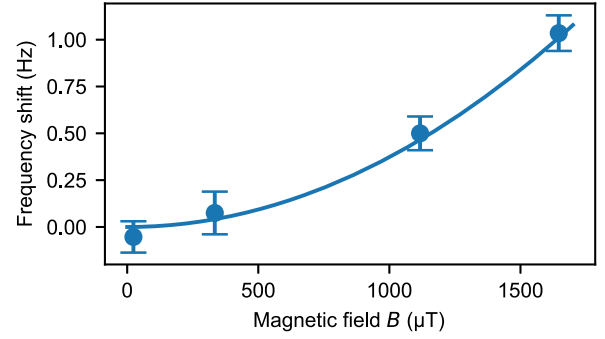


FIG. 3. Measurement of the $m_J = 0 \rightarrow m_{J'} = 0$ clock transition frequency shift in Ca¹⁴⁺ as a function of magnetic field strength B . The fit of the form $\Delta\nu_0 = C_2(0,0)B^2$ yields $C_2(0,0) = 0.39 \pm 0.04 \text{ Hz mT}^{-2}$.

details of the calculations are described in Supplemental Material [20].

The calculated g -factors of the low-lying states in Ca¹⁴⁺ are listed in the last column of Table II. To calculate them, we use the operator for the interaction with the external homogeneous magnetic field \mathbf{B} , which is assumed to be aligned with the z axis:

$$V_m = \mu_z B_z = \frac{ec}{2} \sum_i (\mathbf{r}_i \times \boldsymbol{\alpha}_i)_z B_z, \quad (4)$$

where μ_z is the atomic magnetic moment and α_i is the vector of the Dirac matrices for the i th electron of an ion. The operator in Eq. (4) mixes the large and small components of the wave functions. In this case, negative energy states also contribute [57].

The inclusion of QED effects in the Hamiltonian affects the wave functions and is crucial to obtaining energies that agree with the experiment (cf. Table II). However, this plays a minor role for the g -factors. A much larger contribution to the g -factors comes from the QED corrections to the atomic magnetic moment and can be approximately estimated as an expectation value of the operator

$$\Delta\mu_z = \frac{g_{\text{free}} - 2}{2} \mu_B \sum_i \beta_i \Sigma_{z,i}, \quad (5)$$

where β is the Dirac matrix, $\Sigma_z = \begin{pmatrix} \sigma_z & 0 \\ 0 & \sigma_z \end{pmatrix}$, σ_z is the Pauli matrix, and $g_{\text{free}} = 2[1 + 0.5(\alpha/\pi) - 0.328478... \times (\alpha/\pi)^2 + ...]$ is the free-electron g -factor. A good agreement between this estimate and the rigorous QED calculation was recently demonstrated in boronlike Ar [58]. For Ca¹⁴⁺, the theoretical result for the 3P_1 state $g^{(\text{theo})} = 1.49902$ is in good agreement with the experimental value $g = 1.499032(6)$. We emphasize that the contributions from negative energy eigenstates (-0.00009) and QED corrections to the atomic magnetic moment (0.00116) are critical for achieving agreement. Further calculations

TABLE II. Theoretical energies (in cm^{-1}) and g -factors of $2s^22p^2$ states of Ca^{14+} given relative to the 3P_0 ground-state energy. The contributions of frequency-dependent Breit and QED are given in columns “freq.” and “QED”, respectively. The differences between the final energies with the NIST and Ref. [56] data are given in columns Δ^a and Δ^b , respectively. g -factors are given in the last column.

Level	CI	Freq.	QED	Final	Δ^a	Δ^b	g -factor
3P_1	17 507	−10	60	17 557	−2	1	1.49 902
3P_2	35 839	−17	99	35 921	−2	9	1.47 075
1D_2	108 555	−18	111	108 648	48		1.02 575
1S_0	197 726	−21	52	197 757	87		

should include the rigorous QED treatment and nuclear recoil corrections.

The calculation of C_2 is directly related to the second-order Zeeman coefficients $g_g^{(2)}$ and $g_e^{(2)}$ of the ground- and excited-ionic sublevels, following Eq. (2). For a particular sublevel $|\Gamma J m_J\rangle$, these dimensionless coefficients can be obtained within second-order perturbation theory as

$$g^{(2)}(m_J) = \frac{m_e c^2}{\mu_B^2} \sum_{\Gamma' J'} \frac{|\langle \Gamma' J' m_J | \mu_z + \Delta \mu_z | \Gamma J m_J \rangle|^2}{E(\Gamma J) - E(\Gamma' J')}, \quad (6)$$

where the operators μ_z and $\Delta \mu_z$ are given by Eqs. (4) and (5), respectively. J is the total angular momentum, and Γ represents the set of all other quantum numbers necessary for a unique specification of the state. Moreover, the intermediate state summation $\sum_{\Gamma' J'}$ runs over all states with energies $E(\Gamma' J') \neq E(\Gamma J)$. For computational purposes, this summation was restricted to energetically near fine-structure states 3P_0 , 3P_1 , 3P_2 , 1D_2 , and 1S_0 , belonging to the reference electronic configuration $2s^22p^2$. Moreover, the matrix elements in Eq. (6) were obtained using the multiconfiguration Dirac-Fock (MCDF) approach. Based on MCDF calculations, we obtained the theoretical prediction $C_2^{(\text{theo})}(0,0) = 0.3730(3) \text{ Hz/mT}^{-2}$ [59], which is in good agreement with the experimental value $C_2(0,0) = 0.39(4) \text{ Hz/mT}^{-2}$. To our knowledge, this is the first experimental confirmation of a theoretically calculated C_2 in HCl.

Conclusions—In this Letter, we have investigated the response of the atomic structure of carbonlike Ca^{14+} to magnetic fields through microwave and optical spectroscopy. We measured the g -factor of the excited-state 3P_1 with a relative uncertainty of 4×10^{-6} . The state-of-the-art calculations show a good agreement between experiment and theory, highlighting the significance of QED contributions in the g -factor of few-electron systems, which have been largely unexplored in experimental studies. Furthermore, we determined the second-order Zeeman shift coefficient $C_2(0,0)$, which, to the best of our knowledge, is the smallest value

reported to date. This proves the long-standing theoretical prediction that HCl are highly insensitive to external magnetic fields [16] and advances the work toward the development of next-generation optical clocks employing HCl. The experimental methods employed in this Letter are transferable to a wide range of HCl with an optical transition suitable for quantum logic spectroscopy [2]. This includes hydrogenlike systems in heavy HCl [60], where the ground-state g -factor currently provides the most stringent test of strong-field QED [4].

Acknowledgments—We thank Mikhail Kozlov for bringing our attention to the potentially significant effect of the frequency-dependent Breit and subsequent fruitful discussions. We thank Ilya Tupitsyn and Dmitry Glazov for fruitful discussions regarding frequency-dependent Breit contributions and g -factor calculations. We thank Vladimir Yerokhin for computing the effect of the frequency-dependent Breit interaction in Li-like Ca, which demonstrated that the effect may be significant. We thank Daniele Nicolodi, Thomas Legero, and Uwe Sterr for providing the ultrastable Si cavity as a laser reference. The project was supported by the Physikalisch-Technische Bundesanstalt, the Max-Planck Society, the Max-Planck-Riken-PTB-Center for Time, Constants and Fundamental Symmetries, and the Deutsche Forschungsgemeinschaft (DFG, German Research Foundation) through SCHM2678/5-2, SU 658/4-2, the collaborative research centers SFB 1225 ISOQUANT and SFB 1227 DQ-mat, and under Germany’s Excellence Strategy—EXC-2123 QuantumFrontiers—390837967. The project 20FUN01 TSCAC has received funding from the EMPIR program cofinanced by the Participating States and from the European Union’s Horizon 2020 research and innovation program. This project has received funding from the European Research Council (ERC) under the European Union’s Horizon 2020 research and innovation program (Grant Agreement No. 101019987). The theoretical work has been supported in part by the U.S. NSF Grant No. PHY-2309254, U.S. Office of Naval Research Grant No. N00014-20-1-2513, and European Research Council (ERC) under the Horizon 2020 Research and Innovation Program of the European Union (Grant Agreement No. 856415). The calculations in this work were done through the use of Information Technologies resources at the University of Delaware, specifically the high-performance Caviness and DARWIN computer clusters.

Data availability—The data are available from the authors upon reasonable request.

- [1] M. S. Safronova, D. Budker, D. DeMille, Derek F. Jackson Kimball, A. Derevianko, and C. W. Clark, *Rev. Mod. Phys.* **90**, 025008 (2018).
- [2] M. G. Kozlov, M. S. Safronova, J. R. Crespo López-Urrutia, and P. O. Schmidt, *Rev. Mod. Phys.* **90**, 045005 (2018).

- [3] K. Blaum, S. Eliseev, and S. Sturm, *Quantum Sci. Technol.* **6**, 014002 (2020).
- [4] J. Morgner, B. Tu, C. M. König, T. Sailer, F. Heiße, H. Bekker, B. Sikora, C. Lyu, V. A. Yerokhin, Z. Harman, J. R. Crespo López-Urrutia, C. H. Keitel, S. Sturm, and K. Blaum, *Nature (London)* **622**, 53 (2023).
- [5] T. Sailer, V. Debievre, Z. Harman, F. Heiße, C. König, J. Morgner, B. Tu, A. V. Volotka, C. H. Keitel, K. Blaum, and S. Sturm, *Nature (London)* **606**, 479 (2022).
- [6] F. Heiße, M. Door, T. Sailer, P. Filianin, J. Herkenhoff, C. M. König, K. Kromer, D. Lange, J. Morgner, A. Rischka, Ch. Schweiger, B. Tu, Y. N. Novikov, S. Eliseev, S. Sturm, and K. Blaum, *Phys. Rev. Lett.* **131**, 253002 (2023).
- [7] A. Wagner, S. Sturm, F. Köhler, D. A. Glazov, A. V. Volotka, G. Plunien, W. Quint, G. Werth, V. M. Shabaev, and K. Blaum, *Phys. Rev. Lett.* **110**, 033003 (2013).
- [8] D. von Lindenfels, M. Wiesel, D. A. Glazov, A. V. Volotka, M. M. Sokolov, V. M. Shabaev, G. Plunien, W. Quint, G. Birkel, A. Martin, and M. Vogel, *Phys. Rev. A* **87**, 023412 (2013).
- [9] N.-H. Rehbehn, M. K. Rosner, H. Bekker, J. C. Berengut, P. O. Schmidt, S. A. King, P. Micke, M. F. Gu, R. Müller, A. Surzhykov, and J. R. Crespo López-Urrutia, *Phys. Rev. A* **103**, L040801 (2021).
- [10] R. Soria Orts, J. R. Crespo López-Urrutia, H. Bruhns, A. J. González Martínez, Z. Harman, U. D. Jentschura, C. H. Keitel, A. Lapiere, H. Tawara, I. I. Tupitsyn, J. Ullrich, and A. V. Volotka, *Phys. Rev. A* **76**, 052501 (2007).
- [11] S. A. King, L. J. Spieß, P. Micke, A. Wilzewski, T. Leopold, E. Benkler, R. Lange, N. Huntemann, A. Surzhykov, V. A. Yerokhin, J. R. Crespo López-Urrutia, and P. O. Schmidt, *Nature (London)* **611**, 43 (2022).
- [12] P. Micke, T. Leopold, S. A. King, E. Benkler, L. J. Spieß, L. Schmöger, M. Schwarz, J. R. Crespo López-Urrutia, and P. O. Schmidt, *Nature (London)* **578**, 60 (2020).
- [13] I. Arapoglou, A. Egl, M. Höcker, T. Sailer, B. Tu, A. Weigel, R. Wolf, H. Cakir, V. A. Yerokhin, N. S. Oreshkina, V. A. Agababae, A. V. Volotka, D. V. Zinenko, D. A. Glazov, Z. Harman, C. H. Keitel, S. Sturm, and K. Blaum, *Phys. Rev. Lett.* **122**, 253001 (2019).
- [14] J. E. Bernard, L. Marmet, and A. A. Madej, *Opt. Commun.* **150**, 170 (1998).
- [15] W. M. Itano, *J. Res. NIST* **105**, 829 (2000).
- [16] J. C. Berengut, V. A. Dzuba, V. V. Flambaum, and A. Ong, *Phys. Rev. A* **86**, 022517 (2012).
- [17] T. Rosenband, P. O. Schmidt, D. B. Hume, W. M. Itano, T. M. Fortier, J. E. Stalnaker, K. Kim, S. A. Diddams, J. C. J. Koelemeij, J. C. Bergquist, and D. J. Wineland, *Phys. Rev. Lett.* **98**, 220801 (2007).
- [18] T. Leopold, S. A. King, P. Micke, A. Bautista-Salvador, J. C. Heip, C. Ospelkaus, J. R. Crespo López-Urrutia, and P. O. Schmidt, *Rev. Sci. Instrum.* **90**, 073201 (2019).
- [19] P. Micke, J. Stark, S. A. King, T. Leopold, T. Pfeifer, L. Schmöger, M. Schwarz, L. J. Spieß, P. O. Schmidt, and J. R. Crespo López-Urrutia, *Rev. Sci. Instrum.* **90**, 065104 (2019).
- [20] See Supplemental Material at <http://link.aps.org/supplemental/10.1103/p88p-brnx> for details about motional frequency measurements, which also includes Refs. [21–23]; details about equations for the calculations of ion distance d , which also includes Refs. [24–26]; and details for the theoretical calculations about g -factor, which also includes Refs. [27–38].
- [21] D. J. Heinzen and D. J. Wineland, *Phys. Rev. A* **42**, 2977 (1990).
- [22] K. C. McCormick, J. Keller, D. J. Wineland, A. C. Wilson, and D. Leibfried, *Quantum Sci. Technol.* **4**, 024010 (2019).
- [23] C. Wunderlich, T. Hannemann, T. Körber, H. Häffner, C. Roos, W. Hänsel, R. Blatt, and F. Schmidt-Kaler, *J. Mod. Opt.* **54**, 1541 (2007).
- [24] D. F. V. James, *Appl. Phys. B* **66**, 181 (1998).
- [25] D. Kielpinski, B. E. King, C. J. Myatt, C. A. Sackett, Q. A. Turchette, W. M. Itano, C. Monroe, D. J. Wineland, and W. H. Zurek, *Phys. Rev. A* **61**, 032310 (2000).
- [26] J. P. Home, D. Hanneke, J. D. Jost, D. Leibfried, and D. J. Wineland, *New J. Phys.* **13**, 073026 (2011).
- [27] E. Tiesinga, P. J. Mohr, D. B. Newell, and B. N. Taylor, *Rev. Mod. Phys.* **93**, 025010 (2021).
- [28] S. Verdebout, C. Nazé, P. Jönsson, P. Rynkun, M. Godefroid, and G. Gaigalas, *At. Data Nucl. Data Tables* **100**, 1111 (2014).
- [29] J. B. Mann and W. R. Johnson, *Phys. Rev. A* **4**, 41 (1971).
- [30] M. H. Mittleman, *Phys. Rev. A* **5**, 2395 (1972).
- [31] I. P. Grant and N. C. Pyper, *J. Phys. B* **9**, 761 (1976).
- [32] I. I. Tupitsyn, S. V. Bezborodov, A. V. Malyshev, D. V. Mironova, and V. M. Shabaev, *Opt. Spectrosc.* **128**, 21 (2020).
- [33] M. S. Safronova, V. A. Dzuba, V. V. Flambaum, U. I. Safronova, S. G. Porsev, and M. G. Kozlov, *Phys. Rev. A* **90**, 042513 (2014).
- [34] M. S. Safronova, V. A. Dzuba, V. V. Flambaum, U. I. Safronova, S. G. Porsev, and M. G. Kozlov, *Phys. Rev. A* **90**, 052509 (2014).
- [35] D. V. Zinenko, D. A. Glazov, V. P. Kosheleva, A. V. Volotka, and S. Fritzsche, *Phys. Rev. A* **107**, 032815 (2023).
- [36] S. G. Porsev, M. G. Kozlov, and M. S. Safronova, *Phys. Rev. A* **108**, L051102 (2023).
- [37] F.-F. Wu, T.-Y. Shi, W.-T. Ni, and L.-Y. Tang, *Phys. Rev. A* **108**, L051101 (2023).
- [38] Yu. Ralchenko, A. Kramida, and J. Reader (The NIST ASD Team), NIST Atomic Spectra Database, National Institute of Standards and Technology, Gaithersburg, MD, Available at <http://physics.nist.gov/asd>.
- [39] D. J. Wineland, J. J. Bollinger, and W. M. Itano, *Phys. Rev. Lett.* **50**, 628 (1983).
- [40] N. Shiga, W. M. Itano, and J. J. Bollinger, *Phys. Rev. A* **84**, 012510 (2011).
- [41] P. Micke, S. Kühn, L. Buchauer, J. R. Harries, T. M. Bücking, K. Blaum, A. Cieluch, A. Egl, D. Hollain, S. Kraemer, T. Pfeifer, P. O. Schmidt, R. X. Schüssler, C. Schweiger, T. Stöhlker, S. Sturm, R. N. Wolf, S. Bernitt, and J. R. Crespo López-Urrutia, *Rev. Sci. Instrum.* **89**, 063109 (2018).
- [42] A. Wilzewski *et al.*, *Phys. Rev. Lett.* **134**, 233002 (2025).
- [43] L. Schmöger, O. O. Versolato, M. Schwarz, M. Kohnen, A. Windberger, B. Piess, S. Feuchtenbeiner, J. Pedregosa-Gutierrez, T. Leopold, P. Micke, A. K. Hansen, T. M. Baumann, M. Drewsen, J. Ullrich, P. O. Schmidt, and J. R. Crespo López-Urrutia, *Science* **347**, 1233 (2015).

- [44] P. O. Schmidt, T. Rosenband, C. Langer, W. M. Itano, J. C. Bergquist, and D. J. Wineland, *Science* **309**, 749 (2005).
- [45] J. Stenger, H. Schnatz, C. Tamm, and H. R. Telle, *Phys. Rev. Lett.* **88**, 073601 (2002).
- [46] D. G. Matei, T. Legero, S. Häfner, C. Grebing, R. Weyrich, W. Zhang, L. Sonderhouse, J. M. Robinson, J. Ye, F. Riehle, and U. Sterr, *Phys. Rev. Lett.* **118**, 263202 (2017).
- [47] M. D. Barrett, B. DeMarco, T. Schaetz, V. Meyer, D. Leibfried, J. Britton, J. Chiaverini, W. M. Itano, B. Jelenković, J. D. Jost, C. Langer, T. Rosenband, and D. J. Wineland, *Phys. Rev. A* **68**, 042302 (2003).
- [48] S. Chen, L. J. Spieß, A. Wilzewski, M. Wehrheim, J. R. Crespo López-Urrutia, and P. O. Schmidt (to be published).
- [49] H. C. J. Gan, G. Maslennikov, K.-W. Tseng, T. R. Tan, R. Kaewuam, K. J. Arnold, D. Matsukevich, and M. D. Barrett, *Phys. Rev. A* **98**, 032514 (2018).
- [50] K. J. Arnold, R. Kaewuam, S. R. Chanu, T. R. Tan, Z. Zhang, and M. D. Barrett, *Phys. Rev. Lett.* **124**, 193001 (2020).
- [51] N. Huntemann, C. Sanner, B. Lipphardt, C. Tamm, and E. Peik, *Phys. Rev. Lett.* **116**, 063001 (2016).
- [52] C. Cheung, M. Safronova, and S. Porsev, *Symmetry* **13**, 621 (2021).
- [53] C. Shah, M. Togawa, M. Botz, J. Danisch, J. Goes, S. Bernitt, M. Maxton, K. Köbnick, J. Buck, J. Selmann, M. Hoesch, M. Gu, F. Porter, T. Pfeifer, M. A. Leutenegger, C. Cheung, M. S. Safronova, and J. R. Crespo López-Urrutia, *Astrophys. J.* **969**, 52 (2024).
- [54] C. Cheung, M. G. Kozlov, S. G. Porsev, M. S. Safronova, I. I. Tupitsyn, and A. I. Bondarev, *Comput. Phys. Commun.* **308**, 109463 (2025).
- [55] I. I. Tupitsyn, M. G. Kozlov, M. S. Safronova, V. M. Shabaev, and V. A. Dzuba, *Phys. Rev. Lett.* **117**, 253001 (2016).
- [56] N.-H. Rehbehn, M. K. Rosner, H. Bekker, J. C. Berengut, P. O. Schmidt, S. A. King, P. Micke, M. F. Gu, R. Müller, A. Surzhykov, and J. R. Crespo López-Urrutia, *Phys. Rev. A* **103**, L040801 (2021).
- [57] E. Lindroth and A. Ynnerman, *Phys. Rev. A* **47**, 961 (1993).
- [58] D. E. Maison, L. V. Skripnikov, and D. A. Glazov, *Phys. Rev. A* **99**, 042506 (2019).
- [59] J. Gilles, S. Fritzsche, L. J. Spieß, P. O. Schmidt, and A. Surzhykov, *Phys. Rev. A* **110**, 052812 (2024).
- [60] S. Schiller, *Phys. Rev. Lett.* **98**, 180801 (2007).